

Cooperative Multi-Robot Localization under Communication Constraints

Nikolas Trawny, Stergios I. Roumeliotis, and Georgios B. Giannakis

Abstract—This paper addresses the problem of cooperative localization (CL) under severe communication constraints. Specifically, we present minimum mean square error (MMSE) and maximum a posteriori (MAP) estimators that can process measurements quantized with as little as one bit per measurement. During CL, each robot quantizes and broadcasts its measurements and receives the quantized observations of its teammates. The quantization process is based on the appropriate selection of thresholds, computed using the current state estimates, that minimize the estimation error metric considered. Extensive simulations demonstrate that the proposed Iteratively-Quantized Extended Kalman filter (IQEKF) and the Iteratively Quantized MAP (IQMAP) estimator achieve performance indistinguishable of that of their real-valued counterparts (EKF and MAP, respectively) when using as few as 4 bits for quantizing each robot measurement.

I. INTRODUCTION

Networks of mobile robots have recently been proposed for tasks such as aerial surveillance [1], search and rescue operations [2], underwater- [3] or even space exploration [4]. For any robotic task, accurate localization, i.e., determining the position and orientation (pose) of each robot, is a fundamental requirement. In contrast to the simple solution of localizing each robot in a team independently, cooperative localization (CL) [5], [6], [7] incorporates robot-to-robot observations and *jointly* estimates all robots' poses, which significantly improves localization accuracy for all team members [8]. Unfortunately, this benefit comes at the cost of increased computation and communication.

Recent research has focussed primarily on reducing the *computational requirements* of CL (e.g., [9], [10], [11], [12]). However, also the *communication requirements* of CL are substantial, since, depending on the approach, either measurements from both proprioceptive and exteroceptive sensors, or state estimates and covariance matrices have to be exchanged. Communicating all these quantities might be infeasible if the robots are subject to communication constraints due to (i) the nature of the *operational environment* (e.g., limited bandwidth caused by strong signal attenuation and perturbation underwater or underground), (ii) the specific *application domain* (e.g., stealth requirements in military operations), or (iii) *economic motivations* (e.g., in

This work was supported by the University of Minnesota (DTC), and the National Science Foundation (EIA-0324864, IIS-0643680, IIS-0811946).

N. Trawny and S. I. Roumeliotis are with the Department of Computer Science and Engineering, University of Minnesota, Minneapolis, MN 55455 (e-mail: {trawny,stergios}@cs.umn.edu)

G. B. Giannakis is with the Department of Electrical and Computer Engineering, University of Minnesota, Minneapolis, MN 55455 (e-mail: georgios@ece.umn.edu)

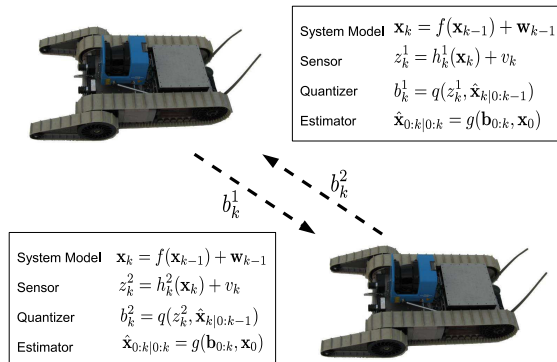


Fig. 1. Multi-centralized, cooperative localization using quantized measurements with two robots. At every time step k , each robot i quantizes its measurements (e.g., linear and rotational velocity, robot-to-robot distance and bearing) and broadcasts the resulting bit sequences, \mathbf{b}_k^i , to its partners. Every robot computes the same estimate, $\hat{\mathbf{x}}_{0:k|0:k}$, of the pose of the entire team, based on all quantized measurements available up to time step k , as well as on shared knowledge of system- and measurement model and their associated noise characteristics.

order to extend the operational life-span through lower power consumption resulting from reduced data transmissions).

In this paper, we investigate algorithms that can perform CL with significantly reduced communication, by transmitting (severely) quantized instead of real-valued sensor observations.¹ For this purpose, we present a minimum mean square error (MMSE) filter [13] and derive a new maximum a posteriori (MAP) batch estimator specifically designed for dynamic random process estimation with quantized observations. We show that, despite significantly reduced communication requirements, their performance in CL comes very close to that of real-valued estimators. In particular, we propose a “multi-centralized” system (cf. Fig. 1), where each robot executes the exact same estimation algorithm, and broadcasts its quantized observations to all other robots. Combined with the shared knowledge of system- and sensor models, each robot is able to compute the same quantization thresholds and the same estimate.

The contributions of this paper are twofold: (i) we develop for the first time single- and multi-bit MAP estimators for estimation of random processes with quantized observations, and (ii) apply quantized filter and MAP algorithms as a

¹In digital systems, real-valued scalars are usually already generically quantized, e.g., with 32 or 64 bits. However, we consider the case of severe and adaptive quantization with 1-to- N bits, optimized for the case of estimation.

novel solution to the problem of multi-robot cooperative localization under communication constraints.

After a brief review of the related literature (Section II) we present the MMSE (Section III) and MAP algorithms (Section IV), demonstrate their performance in simulation (Section V), and conclude the paper with an outlook on future work (Section VI).

II. RELATED WORK

A. Cooperative Localization

The idea of CL – exploiting robot-to-robot measurements, and concurrently estimating the pose of the entire robot team in order to improve localization accuracy – has been subject of active research in the recent past. A variety of algorithms have been proposed for CL, among them Maximum Likelihood estimation (MLE) [6], or extended Kalman filter (EKF)-based approaches [7]. Several strategies aim at reducing the communication and computational complexity of CL, for example distributed implementations [7], [12], approximations based on decoupling [9], [10], hierarchical group division [11], or sensor scheduling [14]. The drawbacks of these approaches are suboptimal or overconfident estimates due to neglected correlations as in [9], [10], [11], that some measurements have to be entirely discarded in order to fit the communication constraints [14], or that the algorithm is incapable of adaptively adjusting to bandwidth variability [7], [12]. By considering quantized measurements, our proposed algorithms can trade off estimation accuracy for bandwidth requirements, and thus react to varying communication constraints.

B. Estimation with quantized observations

In their regular form, the classic estimation techniques used in CL (e.g., EKF or MLE) rely on real-valued measurements and cannot address estimation with quantized observations. The latter has recently received growing interest in the signal processing community. Early work on quantized estimation was concerned with estimating *constant parameters*, e.g., based on noisy sensor observations that were quantized and transmitted to a fusion center [15]. Several studies have investigated the loss of performance compared to real-valued estimation, for example for MLE [16] or for MAP estimators [17].

In contrast, few approaches exist for the problem of *dynamic random process estimation* using quantized observations. Ribeiro *et al.* [18] developed a filtering scheme (sign-of-innovation Kalman filter or SOI-KF) for scalar observations of a linear Gaussian random process, quantized with one bit per measurement. By approximating the posterior probability density function (pdf) as a Gaussian after each update, they achieved a filter structure very similar to that of the regular Kalman filter. Msechu *et al.* [13] extended this approach to observations quantized with multiple bits (iteratively quantized Kalman filter or IQKF). Despite the significant reduction in communication, the performance of both SOI-KF and IQKF comes surprisingly close to that of the real-valued KF. At the same time, SOI-KF and IQKF are

examples of “multi-centralized” estimators, where all sensors share the same estimate. This structure eliminates the fusion center, which can be a single-point of failure. We will discuss these filtering algorithms in more detail in Section III-B.

For nonlinear problems (e.g., CL in 2D), linearized estimators such as the EKF (or, correspondingly, SOI-EKF and IQEKF) are suboptimal for two reasons: First, they repeatedly treat non-Gaussian pdfs as Gaussians, and second, they approximate the nonlinear system and measurement models by their first-order Taylor series expansion. It is known from real-valued estimation, that batch MAP estimators can mitigate these issues. With the same objective in mind, in this paper we develop MAP estimators for estimating dynamic random processes with quantized observations. In particular, we introduce the single-bit quantized MAP (QMAP) and the iteratively quantized, multi-bit MAP (IQMAP) algorithms.

III. MMSE ESTIMATION

Let us assume a discrete-time, linear dynamic system with M_k scalar measurements per time step

$$\mathbf{x}_k = \mathbf{F}_{k-1}\mathbf{x}_{k-1} + \mathbf{G}_{k-1}\mathbf{w}_{k-1}, \quad \mathbf{x}_0 \sim \mathcal{N}(\mathbf{x}_{\text{ini}}, \mathbf{P}_0) \quad (1)$$

$$z_{km} = \mathbf{h}_{km}^T \mathbf{x}_k + v_{km}, \quad m = 1, \dots, M_k \quad (2)$$

with zero-mean, white Gaussian, uncorrelated system and measurement noise with covariance

$$E[\mathbf{w}_k \mathbf{w}_l^T] = \delta_{kl} \mathbf{Q}_k, \quad E[v_{km} v_{ln}] = \delta_{km,ln} \sigma_{km}^2 \quad (3)$$

Notice that in this formulation the only control input is system noise. Usually in mobile robotics, the system dynamics are given by a kinematic model, with velocity or acceleration measurements acting as control input. Here, we assume instead a statistical motion model (e.g., zero acceleration driven by white noise [19]), allowing us to include the control variables (e.g., linear and rotational velocities) in the state vector. As a consequence, measurements from proprioceptive and exteroceptive sensors can be treated identically. Notice further that this formulation also allows vector-valued measurements, since these can be decomposed into several scalar measurements after appropriate pre-whitening. Finally, we note that the linear formulation (1)-(3) is used to render the following derivations mathematically tractable. Later on, we will use linearization to accommodate the *nonlinear* system and measurement models prevalent in robotics.

A. Kalman Filter

It is well known that the optimal MMSE estimate of the state \mathbf{x}_k given all measurements up to time step k (denoted as $\hat{\mathbf{x}}_{k|k}$ and $\mathbf{z}_{0:k}$, respectively) is the conditional mean of the posterior pdf $p[\mathbf{x}_k | \mathbf{z}_{0:k}]$

$$\hat{\mathbf{x}}_{k|k} := E[\mathbf{x}_k | \mathbf{z}_{0:k}] = \int_{-\infty}^{\infty} \mathbf{x}_k p[\mathbf{x}_k | \mathbf{z}_{0:k}] d\mathbf{x}_k \quad (4)$$

For a linear system with Gaussian noise, both the prior and the posterior pdf are Gaussian, and hence are completely characterized by the mean $\hat{\mathbf{x}}$ and the covariance \mathbf{P} . Both are computed by the regular Kalman filter, described in Algorithm 1. Notice that the state update requires knowledge of the (real-valued) measurement z_{km} .

Algorithm 1 Kalman filter

1: KF Propagation

$$\hat{\mathbf{x}}_{k|k-1} = \mathbf{F}_{k-1} \hat{\mathbf{x}}_{k-1|k-1}$$
$$\mathbf{P}_{k|k-1} = \mathbf{F}_{k-1} \mathbf{P}_{k-1|k-1} \mathbf{F}_{k-1}^T + \mathbf{G}_{k-1} \mathbf{Q}_{k-1} \mathbf{G}_{k-1}^T$$

2: KF Measurement Update, $m = 1, \dots, M_k$

$$\hat{\mathbf{x}}_{k|k,m} = \hat{\mathbf{x}}_{k|k,m-1}$$
$$+ \frac{\mathbf{P}_{k|k,m-1} \mathbf{h}_{km}}{\mathbf{h}_{km}^T \mathbf{P}_{k|k,m-1} \mathbf{h}_{km} + \sigma_{km}^2} (z_{km} - \mathbf{h}_{km}^T \hat{\mathbf{x}}_{k|k,m-1})$$
$$\mathbf{P}_{k|k,m} = \mathbf{P}_{k|k,m-1} - \frac{\mathbf{P}_{k|k,m-1} \mathbf{h}_{km} \mathbf{h}_{km}^T \mathbf{P}_{k|k,m-1}}{\mathbf{h}_{km}^T \mathbf{P}_{k|k,m-1} \mathbf{h}_{km} + \sigma_{km}^2}$$
$$\hat{\mathbf{x}}_{k|k,0} := \hat{\mathbf{x}}_{k|k-1}, \hat{\mathbf{x}}_{k|k} := \hat{\mathbf{x}}_{k|k, M_k}, \mathbf{P}_{k|k,0} := \mathbf{P}_{k|k-1}, \mathbf{P}_{k|k} := \mathbf{P}_{k|k, M_k}$$

B. Single- and Multi-bit Kalman filter (SOI-KF and IQKF)

Assume now, that due to communication constraints we cannot afford to transmit the entire measurement z_{km} , but only a quantized version b_{km} . Further, assume that each robot can broadcast its quantized measurements to all other robots (i.e., by transmitting at a fixed frequency, or in a round-robin fashion), and that error-correcting codes ensure error-free transmission². Finally, assume known system-, measurement-, and noise models, and a commonly shared state estimate throughout the entire network. The last assumption is guaranteed by requiring each member of the network to execute the *same* estimation algorithm using the *same* quantized observations (a process we refer to as “multi-centralized” estimation). As a result, every robot is able to reproduce the quantization thresholds used by the other robots, since they are uniquely determined based on the shared estimate [18].

Algorithm 2 SOI-KF

1: SOI-KF Propagation \equiv KF Propagation (cf. Alg. 1)

2: SOI-KF Quantization Rule

$$b_{km} = \begin{cases} +1 & \text{if } z_{km} - \mathbf{h}_{km}^T \hat{\mathbf{x}}_{k|k,m-1} > 0 \\ -1 & \text{otherwise} \end{cases}$$

3: SOI-KF Measurement Update

$$\hat{\mathbf{x}}_{k|k,m} = \hat{\mathbf{x}}_{k|k,m-1}$$
$$+ \frac{\sqrt{2/\pi} \mathbf{P}_{k|k,m-1} \mathbf{h}_{km}}{\sqrt{\mathbf{h}_{km}^T \mathbf{P}_{k|k,m-1} \mathbf{h}_{km} + \sigma_{km}^2}} b_{km}$$
$$\mathbf{P}_{k|k,m} = \mathbf{P}_{k|k,m-1}$$
$$- (2/\pi) \frac{\mathbf{P}_{k|k,m-1} \mathbf{h}_{km} \mathbf{h}_{km}^T \mathbf{P}_{k|k,m-1}}{\mathbf{h}_{km}^T \mathbf{P}_{k|k,m-1} \mathbf{h}_{km} + \sigma_{km}^2}$$

The quantization of the measurements introduces non-linearity into the system, causing the Gaussianity of the

²The specific design of the scheduling and routing algorithms is beyond the scope of this work.

prior and posterior pdfs to break down, even when both system- and measurement models are linear. As a result, exact MMSE estimation in general becomes intractable. However, if the quantized measurement is chosen as the sign of the innovation, and at each time step the posterior pdf $p[\mathbf{x}_k | \mathbf{b}_{0:k}]$ is approximated as Gaussian with mean $\hat{\mathbf{x}}_{k|k}$ and covariance $\mathbf{P}_{k|k}$, then, as shown in [18], the resulting SOI-KF estimator (cf. Algorithm 2) has a form very similar to the classical KF. Remarkably, one can show that in a continuous-time formulation, the performance, in terms of MSE, of the SOI-KF is the same as that of a real-valued KF with $\pi/2$ times larger measurement noise variance [18]. In other words, by transmitting only a single bit instead of a real-valued scalar, one still achieves about 64% of the performance of the regular KF.

More recent work [13] has shown that similar results hold for quantization with more than one bit per measurement. Specifically, the SOI-KF measurement update shown in Algorithm 2 can be repeated for each bit in an iterative fashion, leading to the iteratively quantized KF, or IQKF. The performance is shown to improve with the number of bits, and even for as little as 4 bits, it reaches 98% of the performance of the real-valued KF.³

IV. MAP ESTIMATION

Notice that neither SOI-KF nor IQKF are exact, since they approximate the (non-Gaussian) posterior pdf as Gaussian after every step. For nonlinear systems, the additional linearization of system- and measurement model in the EKF (or, analogously, in the SOI-EKF [18] or IQEKF [13]) will only exacerbate this problem, and lead over time to filter inconsistency. To overcome these limitations, in this section we investigate real-valued and quantized batch MAP estimation. We expect the smoothing effect of batch estimation to mitigate errors arising from linearization and Gaussian approximation.

A batch MAP estimate is the best estimate of the *entire* state history (denoted as $\mathbf{x}_{0:K}$) given all measurements up to time K (denoted as $\mathbf{z}_{0:K}$). Contrary to the MMSE, which is the *mean* of the posterior pdf, the MAP estimate is given by its *mode*. Using Bayes' rule and the Markov property of the dynamic system, we can write the batch MAP estimate as

$$\hat{\mathbf{x}}_{0:K|0:K} = \arg \max p(\mathbf{x}_{0:K} | \mathbf{z}_{0:K})$$
$$= \arg \max \frac{1}{p(\mathbf{z}_{0:K})} p(\mathbf{z}_{0:K} | \mathbf{x}_{0:K}) p(\mathbf{x}_{0:K})$$
$$= \arg \max \prod_{k=0}^K \prod_{m=1}^{M_k} p(z_{km} | \mathbf{x}_k) \prod_{k=0}^{K-1} p(\mathbf{x}_{k+1} | \mathbf{x}_k) \cdot p(\mathbf{x}_0) \quad (5)$$

For the linear system with Gaussian noise (1)-(3), the conditional pdfs in (5) are also Gaussian. After taking the logarithm, the real-valued MAP estimation problem (5) is equivalent to a weighted Least Squares problem, which can be solved using standard techniques.

³In order to properly account for correlations, the state has to be augmented with the measurement noise in this case. For further details, we refer the interested reader to [13].

A. Single-bit quantized MAP estimation (QMAP)

The situation becomes significantly more challenging when replacing real-valued by quantized measurements. For illustrative purposes, we first analyze the case where each measurement is quantized with exactly one bit. Similarly to the SOI-KF, we will compute the quantized measurement using as threshold $z_{\tau_{km}}$ the expected measurement based on the current MAP estimate.

$$b_{km} = \begin{cases} +1 & \text{if } z_{km} - z_{\tau_{km}} > 0 \\ -1 & \text{otherwise} \end{cases} \quad (6)$$

$$z_{\tau_{km}} = \mathbf{h}_{km}^T \hat{\mathbf{x}}_{k|0:k,m-1} \quad (7)$$

For computing the posterior pdf and the MAP estimate as in (5), we will have to determine the quantized measurement likelihoods $p(b_{km}|\mathbf{x}_k)$ instead of $p(z_{km}|\mathbf{x}_k)$. Due to the assumption of Gaussian measurement noise, we can compute these measurement likelihoods in terms of the Gaussian tail probability⁴ as

$$p(b_{km}|\mathbf{x}_k) = Q\left(\frac{b_{km}(z_{\tau_{km}} - \mathbf{h}_{km}^T \mathbf{x}_k)}{\sigma_{km}}\right) \quad (8)$$

$$\begin{aligned} \text{since } p(b_{km} = 1|\mathbf{x}_k) &= \Pr\{z_{km} - z_{\tau_{km}} > 0|\mathbf{x}_k\} \\ &= \Pr\{v_{km} > z_{\tau_{km}} - \mathbf{h}_{km}^T \mathbf{x}_k|\mathbf{x}_k\} \end{aligned}$$

and similarly for $p(b_{km} = -1|\mathbf{x}_k)$. We are now ready to state the main result for the single-bit quantized MAP in the following proposition:

Proposition 1 (Single-Bit Quantized MAP (QMAP)):

Assume the linear model of (1)-(3). If a single bit is allocated per measurement, with a quantization rule as in (6), the posterior pdf is given by

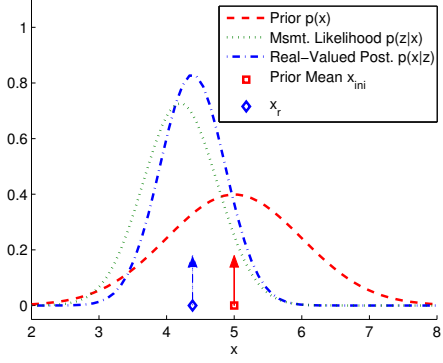
$$\begin{aligned} p(\mathbf{x}_{0:K}|\mathbf{b}_{0:K}) &= \frac{1}{p(\mathbf{b}_{0:K})} \prod_{k=0}^K \prod_{m=1}^{M_k} p(b_{km}|\mathbf{x}_k) \prod_{k=0}^{K-1} p(\mathbf{x}_{k+1}|\mathbf{x}_k) \cdot p(\mathbf{x}_0) \\ &\propto \prod_{k=0}^K \prod_{m=1}^{M_k} Q\left(\frac{b_{km}(z_{\tau_{km}} - \mathbf{h}_{km}^T \mathbf{x}_k)}{\sigma_{km}}\right) \\ &\quad \cdot \prod_{k=0}^{K-1} \mathcal{N}(\mathbf{F}_k \mathbf{x}_k, \mathbf{G}_k \mathbf{Q}_k \mathbf{G}_k^T) \cdot p(\mathbf{x}_0) \end{aligned} \quad (9)$$

The following Lemma is an important consequence of this proposition:

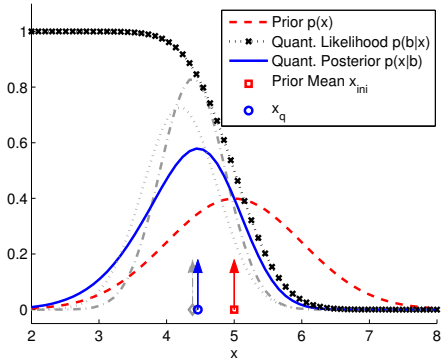
Lemma 1: The posterior pdf of the QMAP given in (9) is log-concave in \mathbf{x} .

This follows from the facts that the Gaussian pdf is log-concave [20], integrals of log-concave pdfs over convex sets are log-concave [21], and log-concavity is closed under multiplication [20]. Log-concavity ensures that the MAP estimate is unique for every choice of $z_{\tau_{km}}$ and can be found using efficient convex optimization techniques [20], which are guaranteed to converge to the global optimum.

Fig. 2 illustrates the difference between real-valued and QMAP estimation for a simple case of a scalar prior, and a single, scalar measurement. Note that while the real-valued posterior is Gaussian, the quantized posterior is skewed and



(a) Pdfs for real-valued estimation, and the corresponding MAP estimate x_r .



(b) Pdfs for quantized estimation, and the corresponding MAP estimate x_q (pdfs for real-valued are shown shaded for comparison).

Fig. 2. Comparison of real-valued and quantized measurement-based posterior pdfs for scalar prior and one scalar measurement $z = x + v$, $x \sim \mathcal{N}(5, 1)$, $v \sim \mathcal{N}(0, 0.3)$, quantized with a single bit. The posterior for the quantized measurement is skewed and heavy-tailed, compared to the real-valued (Gaussian) posterior.

heavy-tailed. However, its log-concavity ensures that the MAP estimate is unique and can be computed efficiently.

B. Multi-bit iteratively quantized MAP estimation (IQMAP)

In case *multiple bits* are available for quantizing a particular measurement, we require an iterative, multi-bit quantization scheme with *adaptive* quantization thresholds. For this purpose, we define the following quantization rule to determine the i th bit allocated to measurement z_{km}

$$b_{km,i} = \begin{cases} +1 & \text{if } z_{km} - z_{\tau_{km,i}} > 0, i = 1, \dots, I \\ -1 & \text{otherwise} \end{cases} \quad (10)$$

We will address how to choose $z_{\tau_{km,i}}$ momentarily.

The idea behind this approach is to define an interval containing z_{km} and iteratively reduce its size. Before receiving the first bit, the measurement z_{km} is known trivially to lie in the interval $-\infty < z_{km} < \infty$. When the first bit arrives, e.g., $b_{km,1} = 1$, we can update this interval to be $z_{\tau_{km,1}} < z_{km} < \infty$. After receiving a sequence of bits $\mathbf{b}_{km} = [b_{km,1} \dots b_{km,I}]$, we can establish successively tighter lower and upper bounds, i.e., $z_{\tau_{km,\ell}} < z_{km} \leq z_{\tau_{km,u}}$, depending on the specific quantization outcomes

⁴Gaussian tail probability $Q(x) := \int_x^\infty (2\pi)^{-1/2} \exp(-u^2/2) du$

and thresholds. In this case, the measurement likelihood of the bit sequence \mathbf{b}_{km} can be computed as $p(\mathbf{b}_{km}|\mathbf{x}_k) = \Pr\{z_{\tau_{km,\ell}} < z_{km} \leq z_{\tau_{km,u}}|\mathbf{x}_k\} = Q\left(\frac{z_{\tau_{km,\ell}} - \mathbf{h}_{km}^T \mathbf{x}_k}{\sigma_{km}}\right) - Q\left(\frac{z_{\tau_{km,u}} - \mathbf{h}_{km}^T \mathbf{x}_k}{\sigma_{km}}\right)$, leading to the following proposition:

Proposition 2 (Iteratively quantized MAP (IQMAP)):

Consider the linear system (1)-(3). If multiple bits are allocated per measurement according to the quantization rule (10), the posterior pdf is given by

$$\begin{aligned} p(\mathbf{x}_{0:K}|\mathbf{b}_{0:K}) &= \frac{1}{p(\mathbf{b}_{0:K})} \prod_{k=0}^{K-1} \prod_{m=1}^{M_k} p(\mathbf{b}_{km}|\mathbf{x}_k) \prod_{k=0}^{K-1} p(\mathbf{x}_{k+1}|\mathbf{x}_k) \cdot p(\mathbf{x}_0) \quad (11) \\ &\propto \prod_{k=0}^{K-1} \prod_{m=1}^{M_k} \left[Q\left(\frac{z_{\tau_{km,\ell}} - \mathbf{h}_{km}^T \mathbf{x}_k}{\sigma_{km}}\right) - Q\left(\frac{z_{\tau_{km,u}} - \mathbf{h}_{km}^T \mathbf{x}_k}{\sigma_{km}}\right) \right] \\ &\quad \cdot \prod_{k=0}^{K-1} \mathcal{N}(\mathbf{F}_k \mathbf{x}_k, \mathbf{G}_k \mathbf{Q}_k \mathbf{G}_k^T) \cdot p(\mathbf{x}_0) \quad (12) \end{aligned}$$

Notice that if the measurements are quantized with a single bit, the IQMAP becomes identical to the QMAP algorithm. Following similar arguments as in the QMAP case (see [22] for details), we also have the following lemma:

Lemma 2: The posterior pdf of the IQMAP, given by (12), is log-concave.

The main difference compared to (9) is the form of the new measurement likelihood, which corresponds to an integral of the Gaussian pdf over a convex set and hence preserves log-concavity [21]. As before, the consequence is that the IQMAP estimate is unique and can be found efficiently.

We now address the question of how to successively select new quantization thresholds. We propose to choose $z_{\tau_{km,i}}$ so that, given all previous quantized observations, the measurement z_{km} could lie on each side of the new threshold with *equal probability*.

Proposition 3 (IQMAP Threshold Selection): Assume measurement z_{km} has been quantized using $i - 1$ bits, yielding lower and upper thresholds $z_{\tau_{km,\ell}}$ and $z_{\tau_{km,u}}$. Further, approximate the conditional pdf $p(z_{km}|\mathbf{b}_{0:k})$ by a Gaussian with mean $\mathbf{h}_{km}^T \hat{\mathbf{x}}_{k|0:k}$ and covariance matrix $\mathbf{h}_{km}^T \mathbf{P}_{k|0:k} \mathbf{h}_{km} + \sigma_{km}^2$, where $\hat{\mathbf{x}}_{k|0:k}$ denotes the current MAP estimate of the state at time step k conditioned on all quantized observations $\mathbf{b}_{0:k}$, and $\mathbf{P}_{k|0:k}$ its covariance, computed from the inverse of the Hessian of (12). (Note that only a small block of this inverse needs to be computed explicitly [22].) The new threshold $z_{\tau_{km,i}}$ that divides the interval between $z_{\tau_{km,\ell}}$ and $z_{\tau_{km,u}}$ into two equiprobable regions can then be computed as

$$\begin{aligned} z_{\tau_{km,i}} &= \mathbf{h}_{km}^T \hat{\mathbf{x}}_{k|0:k} + \sqrt{\mathbf{h}_{km}^T \mathbf{P}_{k|0:k} \mathbf{h}_{km} + \sigma_{km}^2} \\ &\quad \cdot Q^{-1}\left(\frac{1}{2} \left[Q\left(z'_{\tau_{km,\ell}}\right) + Q\left(z'_{\tau_{km,u}}\right) \right]\right) \quad (13) \end{aligned}$$

where $z'_{\tau_{km,*}} := \frac{z_{\tau_{km,*}} - \mathbf{h}_{km}^T \hat{\mathbf{x}}_{k|0:k}}{\sqrt{\mathbf{h}_{km}^T \mathbf{P}_{k|0:k} \mathbf{h}_{km} + \sigma_{km}^2}}$

To see this, we utilize the Gaussian approximation of $p(z_{km}|\mathbf{b}_{0:k})$ to express the probability that z_{km} lies on either

side of the new threshold in terms of the Q -function. The new threshold $z_{\tau_{km,i}}$ should then fulfill

$$\begin{aligned} \Pr\{z_{\tau_{km,\ell}} < z_{km} \leq z_{\tau_{km,i}}|\mathbf{b}_{0:k}\} &= \Pr\{z_{\tau_{km,i}} < z_{km} \leq z_{\tau_{km,u}}|\mathbf{b}_{0:k}\} \\ \Leftrightarrow Q\left(z'_{\tau_{km,\ell}}\right) - Q\left(z'_{\tau_{km,i}}\right) &= Q\left(z'_{\tau_{km,i}}\right) - Q\left(z'_{\tau_{km,u}}\right) \end{aligned}$$

From this, the proposition follows.

V. SIMULATION RESULTS

We tested the IQEKF and the IQMAP for CL with two robots moving in 2D, using the real-valued EKF and MAP as benchmark. The system model for each robot was given by a constant-velocity motion model [19]. The continuous-time dynamics for each robot were given by

$$\dot{\mathbf{x}} = \mathbf{f}(\mathbf{x}) + \mathbf{G}_c \begin{bmatrix} w_V \\ w_\omega \end{bmatrix} \quad (14)$$

with the state defined as $\mathbf{x} = [x \ y \ \phi \ V \ \omega]^T$, $\mathbf{f}(\mathbf{x}) = [V \cos \phi \ V \sin \phi \ \omega \ 0 \ 0]^T$, and $\mathbf{G}_c = [\mathbf{0}_{3 \times 2}^T \ \mathbf{I}_{2 \times 2}]^T$. Further, we chose $\sigma_V = 0.6325 \text{ m/s} \cdot \sqrt{\text{Hz}}$, and $\sigma_\omega = 0.4967 \text{ rad/s} \cdot \sqrt{\text{Hz}}$ as the continuous-time noise standard deviations for the motion model. The simulated trajectories followed these characteristics.

After first-order discretization with time step δt we obtain

$$\mathbf{x}_{k+1} = \mathbf{x}_k + \delta t \mathbf{f}(\mathbf{x}_k) + \mathbf{w}_d \quad (15)$$

with system Jacobian

$$\Phi_k = \begin{bmatrix} 1 & 0 & -V_k \delta t \sin \phi_k & \delta t \cos \phi_k & 0 \\ 0 & 1 & V_k \delta t \cos \phi_k & \delta t \sin \phi_k & 0 \\ 0 & 0 & 1 & 0 & \delta t \\ 0 & 0 & 0 & 1 & 0 \\ 0 & 0 & 0 & 0 & 1 \end{bmatrix}$$

and discrete noise covariance $E[\mathbf{w}_d \mathbf{w}_d^T] = \mathbf{Q}_d$ where

$$\mathbf{Q}_d = \int_{t_k}^{t_{k+1}} \Phi(t_{k+1}, \tau) \mathbf{G}_c \mathbf{Q}_c \mathbf{G}_c^T \Phi(t_{k+1}, \tau)^T d\tau \quad (16)$$

The odometry measurements of linear and rotational velocity, corrupted by zero-mean Gaussian noise with $\sigma_{Vm} = 0.07 \text{ m/s}$ and $\sigma_{\omega m} = 0.28 \text{ rad/s}$, were recorded at 10 Hz and treated as regular measurement updates.

We assumed robot-to-robot distance and bearing measurements at a frequency of 1 Hz, corrupted by additive Gaussian measurement noise with $\sigma_d = 0.05 \text{ m}$ and $\sigma_\theta = 0.09 \text{ rad}$. Notice that none of the robots received absolute position measurements, rendering the system unobservable, with pose estimation errors increasing over time.

We compared the performance of IQEKF and IQMAP with all measurements quantized with 1-4 bits (constant per run) against that of real-valued EKF and MAP in Monte Carlo simulation. The RMS errors are shown in Fig. 3. We can see that the error decreases with increasing number of quantization bits, and that the performance comes close to that of the real-valued estimators with as little as 4 bits per measurements. Moreover, the performance gain per additional bit becomes increasingly small. Both quantized and real-valued MAP estimators perform consistently and considerably better than their filtering counterparts (up to 30% improvement in orientation error), as was expected due

to their ability to mitigate linearization errors in nonlinear problems such as CL. Also, the noticeable sawtooth pattern in the filters, resulting from the 1 Hz robot-to-robot measurements, is effectively smoothed out by the MAP estimators.

A typical result for the estimation error and the corresponding 3σ -bounds for the case of single-bit quantization is shown in Fig. 4. As expected, real-valued MAP outperforms QMAP, which in turn is more accurate than SOI-EKF. However, note the behavior of the quantized filter for the velocity estimate: Since both system and measurement function for this quantity are considered linear by the SOI-EKF, it (wrongly) converges and reaches steady state. The QMAP estimator, however, correctly accounts for the nonlinearity introduced by quantization, and more accurately depicts the evolution of uncertainty, as indicated by the tighter but variable 3σ bounds.

VI. CONCLUSIONS AND FUTURE WORK

In this work, we have derived a new MAP estimator (IQMAP) for estimation of random processes with quantized observations. We have shown its application, as well as that of a quantized filter (IQEKF) [13], to the problem of multi-robot cooperative localization under communication constraints. Compared to the regular encoding using 32 or 64 bits per real scalar measurement, both algorithms can significantly reduce communication requirements by allowing to encode scalar measurements using as little as 1 bit (or more, depending on the available resources).

We have further shown that the IQMAP estimator offers increased accuracy compared to the IQEKF, due to mitigation of linearization errors. For linear systems, finding the IQMAP estimate was shown to be a convex optimization problem, which guarantees a unique solution and allows the use of highly-efficient solvers.

In our future work, we plan to analytically characterize the performance of the quantized MAP estimators in comparison to their real-valued counterparts, which will include provably optimal schemes for selecting the quantization thresholds. We also intend to investigate the IQMAP's ability to efficiently exploit *time-varying* communication resources, by not being forced to spend all available bandwidth (bits) on quantizing the current measurement only (as is the case for the IQEKF), but instead using them to refine pertinent previously quantized measurements. Further directions include analysis and reduction of computational complexity, e.g., by marginalizing out old robot poses. To foster applicability in robotic navigation, we will also focus on the extension to cooperative localization and mapping.

REFERENCES

- [1] R. W. Beard, T. W. McLain, D. B. Nelson, D. Kingston, and D. Johnson, "Decentralized cooperative aerial surveillance using fixed-wing miniature UAVs," *Proceedings of the IEEE*, vol. 94, no. 7, pp. 1306–1324, July 2006.
- [2] H. Sugiyama, T. Tsujioka, and M. Murata, "Collaborative movement of rescue robots for reliable and effective networking in disaster area," in *Proceedings of the International Conference on Collaborative Computing: Networking, Applications and Worksharing*, San Jose, CA, Dec. 19–21, 2005.
- [3] C. J. Cannell and D. J. Stilwell, "A comparison of two approaches for adaptive sampling of environmental processes using autonomous underwater vehicles," in *Proceedings of MTS/IEEE OCEANS*, Washington, DC, Sept. 19–23, 2005, pp. 1514–1521.
- [4] S. B. Kesner, J. S. Plante, P. J. Boston, T. Fabian, and S. Dubowsky, "Mobility and power feasibility of a microbot team system for extraterrestrial cave exploration," in *Proceedings of the IEEE International Conference on Robotics and Automation*, Rome, Italy, Apr. 10–14, 2007, pp. 4893–4898.
- [5] I. M. Rekleitis, G. Dudek, and E. E. Milios, "Multi-robot collaboration for robust exploration," in *Proceedings of the IEEE International Conference on Robotics and Automation*, vol. 4, San Francisco, CA, Apr. 2000, pp. 3164–3169.
- [6] A. Howard, M. J. Mataric, and G. S. Sukhatme, "Localization for mobile robot teams using maximum likelihood estimation," in *Proceedings of the IEEE/RSJ International Conference on Intelligent Robots and Systems*, vol. 1, Lausanne, Switzerland, Sept. 30 – Oct. 4, 2002, pp. 434–439.
- [7] S. I. Roumeliotis and G. A. Bekey, "Distributed multirobot localization," *IEEE Transactions on Robotics and Automation*, vol. 18, no. 5, pp. 781–795, Oct. 2002.
- [8] A. I. Mourikis and S. I. Roumeliotis, "Performance analysis of multirobot cooperative localization," *IEEE Transactions on Robotics*, vol. 22, no. 4, pp. 666–681, Aug. 2006.
- [9] S. Panzieri, F. Pascucci, and R. Setola, "Multirobot localisation using interlaced extended Kalman filter," in *Proceedings of the IEEE/RSJ International Conference on Intelligent Robots and Systems*, Beijing, China, Oct. 9–15, 2006, pp. 2816–2821.
- [10] N. Karam, F. Chausse, R. Aufrère, and R. Chapuis, "Localization of a group of communicating vehicles by state exchange," in *Proceedings of the IEEE/RSJ International Conference on Intelligent Robots and Systems*, Beijing, China, Oct. 9–15, 2006, pp. 519–524.
- [11] A. Martinelli, "Improving the precision on multi robot localization by using a series of filters hierarchically distributed," in *Proceedings of the IEEE/RSJ International Conference on Intelligent Robots and Systems*, San Diego, CA, Oct. 29 – Nov. 2, 2007, pp. 1053–1058.
- [12] E. Nerurkar, S. I. Roumeliotis, and A. Martinelli, "Distributed maximum a posteriori estimation for multi-robot cooperative localization," in *Proceedings of the IEEE International Conference on Robotics and Automation*, Kobe, Japan, May 2009.
- [13] E. J. Msechu, S. I. Roumeliotis, A. Ribeiro, and G. B. Giannakis, "Decentralized quantized Kalman filtering with scalable communication cost," *IEEE Transactions on Signal Processing*, vol. 56, pp. 3727–3741, Aug. 2008.
- [14] A. I. Mourikis and S. I. Roumeliotis, "Optimal sensor scheduling for resource-constrained localization of mobile robot formations," *IEEE Transactions on Robotics*, vol. 22, no. 5, pp. 917–931, Oct. 2006.
- [15] W.-M. Lam and A. R. Reibman, "Design of quantizers for decentralized estimation systems," *IEEE Transactions on Communications*, vol. 41, no. 11, pp. 1602–1605, Nov. 1993.
- [16] H. C. Papadopoulos, G. W. Wornell, and A. V. Oppenheim, "Sequential signal encoding from noisy measurements using quantizers with dynamic bias control," *IEEE Transactions on Information Theory*, vol. 47, no. 3, pp. 978–1002, Mar. 2001.
- [17] F. A. Shah, A. Ribeiro, and G. B. Giannakis, "Bandwidth-constrained MAP estimation for wireless sensor networks," in *Proceedings of the 39th Asilomar Conference on Signals, Systems and Computers*, Pacific Grove, CA, Oct. 30 – Nov. 2, 2005, pp. 215–219.
- [18] A. Ribeiro, G. B. Giannakis, and S. Roumeliotis, "SOI-KF: Distributed Kalman filtering with low-cost communications using the sign of innovations," *IEEE Transactions on Signal Processing*, vol. 54, no. 12, pp. 4782–4795, Dec. 2006.
- [19] Y. Bar-Shalom and X.-R. Li, *Estimation and tracking: principles, techniques, and software*. Norwood, MA: Artech House, Inc., 1993.
- [20] S. Boyd and L. Vandenberghe, *Convex Optimization*. Cambridge University Press, 2004.
- [21] A. Prékopa, "Logarithmic concave measures and related topics," in *Stochastic Programming*, M. A. H. Dempster, Ed. Academic Press, 1980, pp. 63–82.
- [22] N. Trawny and S. Roumeliotis, "Cooperative multi-robot localization under communication constraints," University of Minnesota, Dept. of Comp. Sci. & Eng., MARS Lab, Tech. Rep., 2008.

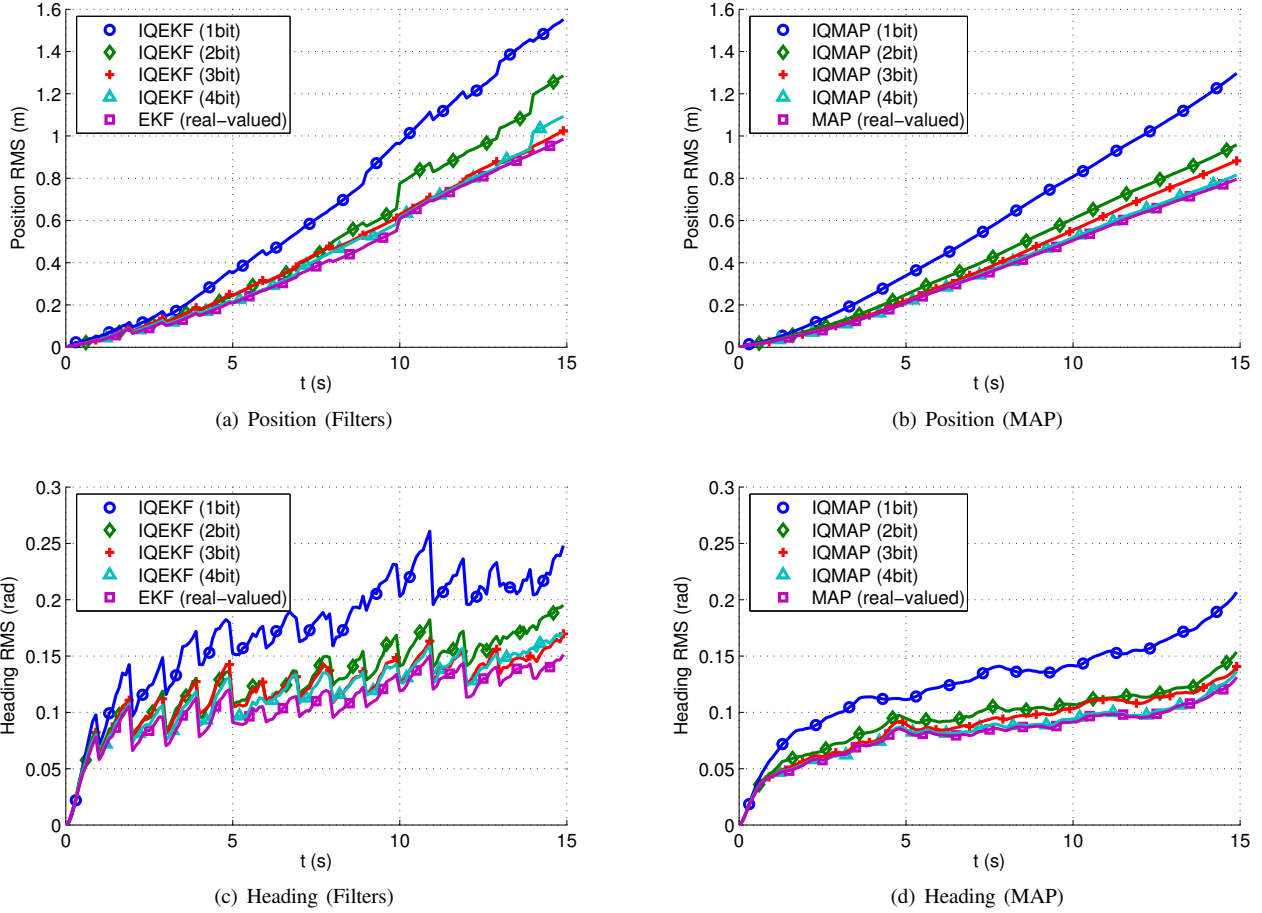


Fig. 3. RMS error for $N_R = 2$ robots and $N_{MC} = 60$ Monte Carlo trials, for EKF, MAP, IQMAP (1-4 bits) and IQEKF (1-4 bits), computed as $RMS(t) = \sqrt{\frac{1}{N_R} \frac{1}{N_{MC}} \sum_{i=1}^{N_R} \sum_{j=1}^{N_{MC}} (\hat{x}_{i,j}(t) - x_{i,j}(t))^2}$.

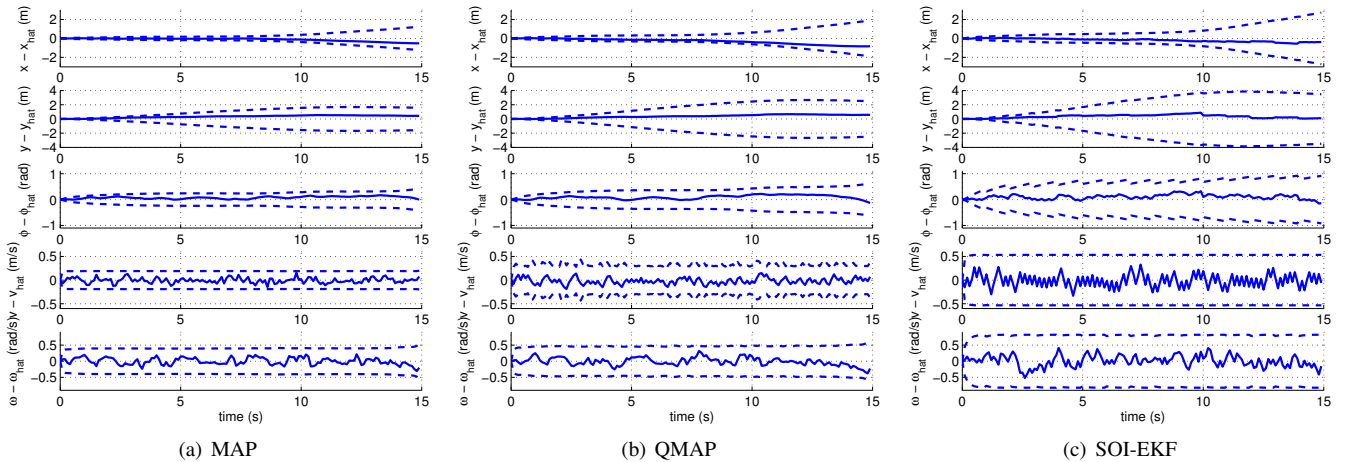


Fig. 4. Typical errors and 3σ -bounds (dashed) for the state estimates of one of the robots, for real-valued MAP, QMAP, and SOI-EKF (one bit). The quantization incurs performance loss (as well as considerable savings in communication). QMAP has better performance than SOI-EKF, showing its ability to better cope with linearization errors. The velocity covariance estimates of the SOI-EKF (but not of the QMAP) wrongly converge to steady state.